Journal of Renewable Materials

Tech Science Press

DOI: 10.32604/jrm.2023.043549

ARTICLE

# Activated Carbon from Nipa Palm Fronds (*Nypa fruticans*) with $H_3PO_4$ and KOH Activators as Fe Adsorbers

**Ninis Hadi Haryanti[1,*], Eka Suarso[1], Tetti N. Manik[1], Suryajaya[1], Nurlita Sari[1] and Darminto[2]**

[1]Physics Study Program, FMIPA, Universitas Lambung Mangkurat, Banjarbaru, 70714, Indonesia

[2]Department of Physics, Institut Teknologi Sepuluh Nopember, Surabaya, 60111, Indonesia

[*]Corresponding Author: Ninis Hadi Haryanti. Email: ninishadiharyanti@ulm.ac.id

Received: 05 July 2023 Accepted: 18 October 2023 Published: 11 March 2024

**ABSTRACT**

Nipa palm is one of the non-wood plants rich in lignocellulosic content. In this study, palm fronds were converted into activated carbon, and their physical, chemical, and morphological properties were characterized. The resulting activated carbon was then applied as an adsorbent of Fe metal in peat water. The carbonization process was carried out for 60 min, followed by sintering at 400°C for 5 h with a particle size of 200 mesh. KOH and $H_3PO_4$ were used in the chemical activation process for 24 h. KOH-activated carbon contained 6.13% of moisture, 4.55% of ash, 17.02% of volatile matter, and 78.84% of fixed carbon, while its Fe reduction efficiency was 28.09%. The $H_3PO_4$-activated carbon contained 4.67% of moisture, 2.84% of ash, 16.41% of volatile matter, and 80.57% of bonded carbon, and the Fe reduction efficiency was 52.25%. KOH-activated carbon and $H_3PO_4$-activated carbon contained fixed carbon of 78.84% and 80.57%, respectively, while their average rates of efficiency of Fe reduction were 22.82% and 39.23%, respectively. Overall, the characteristics of activated nipa carbon met the Indonesian standards (SNI No. 06-3730-1995). However, $H_3PO_4$-activated carbon was found to be better at adsorbing Fe metal from peat water.

**KEYWORDS**

Adsorption; lignocellulosic; reduction of Fe; sintering; volatile content

**Nomenclature**

| | |
|---|---|
| Term 1 | Interpretation 1 |
| Term 2 | Interpretation 2 |

**e.g.,**

| | |
|---|---|
| $\varnothing$ | Porosity |
| $s$ | Skin factor |

## 1 Introduction

According to Global Wetlands data, Indonesia has the second largest peatland in the world with an estimated peatland area of 36,458,236 ha [1]. These peatland are spread across the islands of Sumatra, Kalimantan, and Papua. Peat water in its natural state has a high level of acidity and organic content, so it

does not meet the clean water quality requirements standardized by the Republic of Indonesia Minister of Health Regulation No. 32 of 2017 concerning Sanitation Hygiene [2]. According to Setiasih, peat water contains high levels of Fe, Al, Na, S, and P, while B, Sr, Zn, Cr, Ag, Au, Ca, Ba, Ti, V, Cu, Mn, I, and Co occur in micro quantities [3].

The colour of peat water usually ranges from dark brown to black because it has a fairly high iron content [2]. For treating peat water to make clean water, many methods have been used, such as coagulation [4], electro-coagulation [3], and membrane methods [2]. In water remediation, the heavy metal can be adsorbed using batch [5], phytoremediation [6], and activated carbon methods [7]. The sources of activated carbon are agricultural waste, sewage, municipal waste, industrial waste, forestry residue [8], such as rice straw, bamboo, wood [9], and bagasse [10], which is normally used as an adsorbent for air purification, drinking water, or wastewater because it has a high adsorption capacity. Moreover, the adsorption process also has many advantages, such as high efficiency, low operational cost, and environmental friendliness as it is sourced from biomass that is widely available in nature [11].

Nipa palm (*Nypa fruticans*) is one of the non-timber plants that can grow in mangrove forests. In Indonesia, nipa plants are found in Kalimantan, Sumatra, Maluku, Sulawesi, and Papua. In South Kalimantan, these plants are found in Kotabaru, Tanah Bumbu, Tanah Laut, Hulu Sungai Selatan, and Hulu Sungai Tengah districts [12]. There are many nipa palms in the mangrove forests of South Kalimantan as shown in Fig. 1a. Nipa grows along rivers due to the natural dispersal of the seeds by water. The nipa plants in South Kalimantan are not optimally utilized. Although some parts are used as raw material for making sugar and food ingredients [13] and the leaves are used as roofing for houses [14], nipa fronds (Fig. 1b) are wasted. However, the fronds have the potential to be used as raw material for activated carbon because they contain 48.22% cellulose, 26.4% hemicellulose, and 17.8% lignin [15].

(a) (b)

**Figure 1:** Nipa plants in the mangrove forest of South Kalimantan (a) and Nipa fronds (b)

In general, activated carbon is produced through two stages, namely, carbonization and activation. Carbonization is the process of forming carbon from raw materials, which is carried out at a temperature of 400°C–600°C. The activation process can be carried out in two ways, namely, by means of chemical activation, using alkali metal hydroxides, carbonate salts, chlorides, sulphates, and phosphates from alkaline earth metals and inorganic acids, and physical activation, which involves breaking the carbon chain of the organic compound at 800°C–900°C [9].

Many researchers have prepared activated carbon by using KOH and $H_3PO_4$ as the activating agents [9]. In the case of the nipa plant, the activated carbon produced from nipa palm leaves was used as an adsorbent with adsorption capacities of 59.96% and 96.94% for Fe and Mn, respectively [7], while the activated carbon of nipa palm shell was used as a biosorbent of metal Hg [16]. The adsorption capacity of activated carbon is affected by its particle size, as smaller particle sizes would give better results in adsorption.

According to previous studies, nipa is a locally abundant plant that has a high carbon content and is therefore an appropriate candidate for preparing activated carbon. The process of making activated carbon in this study was adopted from the previous studies. The carbonization of nipa palm fronds was carried out by a simple combustion process for 60 min using the pyrolysis method [17]. Prior to the activation process, the carbon was sintered at 400°C for 5 h [18], which aimed to increase the strength of the carbon and reduce the water content. The activation was carried out using 1 M $H_3PO_4$ and 1 M KOH, which were easily adsorbed on the surface of the activated carbon [19]. The selected particle size was 200 mesh. The activated carbon was then characterized for its surface morphological properties; its elemental content, moisture content, ash content, volatile matter content, and bound carbon were analyzed; and it was applied in the Fe metal content adsorption test in peat water samples.

## 2 Experiment

While the nipa frond samples were taken from Bunipah Village, Banjar Regency, South Kalimantan, peat water samples were taken from the Gambut District, Banjar Regency. Solutions of 1 M $H_3PO_4$ and 1 M KOH were used as activators. $H_3PO_4$ (85% ortho) and KOH were bought from Smart-Lab and LabChem, respectively. Alpha FTIR spectrometer (Bruker), SEM-EDX (Hitachi Flexsem 1000), and cold vapor atomic absorption spectrometer (CV-AAS) instruments were used for various characterizations.

### *2.1 Activated Carbon Preparation and Synthesis*

The nipa frond skin was cut into ±5 cm size and then dried in the sun for 7 days, followed by oven drying at 105°C for 24 h. The frond samples were then carbonized for ±60 min at a temperature of 500°C–800°C using the pyrolysis method in a simple combustion process [17]. The carbonization resulted in charcoal, which was crushed and sieved through a 200-mesh sieve. Then the charcoal powder was sintered at 400°C for 5 h. After the sample was cooled, it was activated by mixing it with 1 M $H_3PO_4$ and 1 M KOH and then rinsing it until the pH value became neutral [20].

### *2.2 Activated Carbon Characterization*

The characteristics of activated carbon including moisture content, ash content, volatile matter content, and fixed carbon content were noted, which met the Indonesian National Standard (SNI) 06-3730-1995. The functional groups were identified with alpha FTIR spectrometer at Chemistry laboratory, Lambung Mangkurat University, Banjarbaru, Indonesia. The metal content was tested using cold vapor atomic absorption spectrometer at the Industrial Research and Standardization Center (BARISTAND), Banjarbaru, Indonesia, and morphological testing was done using a scanning electron microscope (SEM) at Institute Technology of Sepuluh Nopember, Surabaya, Indonesia.

### *2.3 Fe Metal Adsorption Process*

The Fe metal adsorption process was carried out by adding 0.04 grams of nipa-activated carbon in 50 mL of peat water in a closed container and letting it soak for 30 min. After 30 min, the sample was filtered to separate the activated carbon from the peat water. Then the peat water was tested for Fe metal content.

## 3 Results and Discussion

### *3.1 Characteristics of Nipa Palm Frond-Activated Carbon*

Table 1 shows the characteristics of the nipa palm fronds before and after carbonization, sintering, and activation with $H_3PO_4$ and KOH.

As shown in Table 1, the moisture content of the nipa palm fronds before and after carbonization and following sintering consistently decreased. The average moisture content of nipa palm fronds before

carbonization was 12.06%. It was higher than the moisture content of nipa frond fiber reported by Syabana and Widiastuti (2018), which was between 7.4% and 10.1% [21]; this variation may be attributed to regional differences. For activated carbon, the moisture content was 4.81% and 6.27%, respectively, for $H_3PO_4$ and KOH activators. This shows that the presence of an activator can affect the moisture content because the activator can bind water in the activated carbon. This is in accordance with a previous study, in which the carbon activated by $H_3PO_4$ had a moisture content of about 5%, which was lower than that of KOH-activated carbon by about 12% [22].

**Table 1:** Moisture content, ash content, volatile matter, and fixed carbon in nipa frond-activated carbon

| Treatment | Moisture content (%) | Ash content (%) | Volatile matter content (%) | Fixed carbon (%) |
|---|---|---|---|---|
| Before carbonization | 12.06 | 9.79 | 69.78 | 21.63 |
| After carbonization | 6.95 | 8.45 | 16.46 | 75.09 |
| Sintering | 1.13 | 10.54 | 12.10 | 77.35 |
| $H_3PO_4$ | 4.81 | 2.91 | 16.52 | 80.57 |
| KOH | 6.27 | 4.55 | 17.02 | 78.84 |

The ash content before carbonization was still high with a value of 9.79%, while the nipa palm frond samples that had undergone the carbonization process experienced a decrease in ash content due to partial evaporation of the inorganic compounds, with a value of 8.45%. However, the ash content in the sintering process was 10.54%. This increase in ash content could be due to the high sintering temperature and the length of the sintering process. Treatment of the sintering process at 400°C for 5 h can cause many palm frond charcoals to turn into ashes because it has a fragile shape, texture, and fiber structure. On the other hand, the sintering process can remove the impurities contained in the nipa palm charcoal samples due to the oxidation of most of the volatile matter content; however, the ash is not oxidized because it is not a volatile substance. Moreover, the presence of excessive ash content can cause clogging of the pores of activated carbon so that the surface area of the activated carbon is reduced. Table 1 also shows that the ash content was 2.91% on using the $H_3PO_4$ activator, which is lower than that using the KOH activator, i.e., 4.55%. The low ash content can be due to the particle size used in this study, which is 200 meshes. In activated carbon, the ash content should be kept as small as possible because it will reduce its ability to adsorb in the form of both gas and solution. The ash content is also affected by the amount of silica content; the greater the silica content, the larger the ash content that is produced. This was confirmed by the results of the SEM-EDX.

The value of volatile matter content before carbonization was 69.78%, higher than that after carbonization and sintering, which indicate nipa palm frond samples contained impurities. The decrease in the volatile matter content in the sintering process was 12.10%, due to an increase in the combustion temperature in the carbonization and sintering processes, at 400°C for 5 h, so that more and more volatile matter was evaporated [23]. The lowest volatile matter content was 16.52% in the $H_3PO_4$ activation treatment and 17.02% in that of KOH. The value of the volatile matter content as a whole met the maximum SNI standard of 25%. The lowest volatile matter content of activated carbon in $H_3PO_4$ activation was due to its acidic nature, which could expand the surface of activated carbon, thus forming more surfaces. The low level of volatile matter is thought to be due to the evaporation of non-carbon compounds that become volatile during the activation process. These results are in accordance with those in the research conducted by Fauzia and Purnama in 2021 [24], the larger the particle size of the activated carbon, the higher the level of ash content contained in it. The adsorption process for lower ash

content (high volatile matter content) was better than for a higher one because it caused an increase in the surface area.

In Table 1, the value of the carbon content bound to the palm fronds before carbonization, after carbonization, and after sintering increased, respectively, to 21.63%, 75.09% and 77.35%. The fixed carbon value was affected by the ash and volatile matter content; the higher the value of the volatile matter and the ash content, the lower the bonded carbon value became and vice versa [25]. This shows the potential of nipa fronds as raw material for activated carbon. Fixed carbon values once again increased to 80.57% and 78.84% after activation with $H_3PO_4$ and KOH. The results of this study as a whole met the quality standard of activated carbon SNI 6-3730-1995, which stipulates a minimum fixed carbon content of 65%. The high value of fixed carbon indicates the purity of the material in the carbon fraction increased. The increase in fixed carbon content was not only influenced by the ash content and volatile matter content but also by the cellulose and lignin content of materials that could be converted into carbon atoms [8]. These results were confirmed by the FTIR test.

### *3.2 Analysis of Morphology and Elemental Content of Activated Carbon*

The surface morphological structure of the fronds at 500× magnification is shown in Fig. 2a and after carbonization and activation with KOH and H3PO4, respectively, in Figs. 2b–2d, each with a 2000× magnification. Fig. 2a shows that the starting material of nipa fronds with a 500× magnification had a round pore shape with very small holes. The surface of the sample in Fig. 2b after carbonization shows changes in the pores of the activated carbon. The evaporation of cellulose components and water vapor when heated caused rough and irregular pore surfaces to be formed.

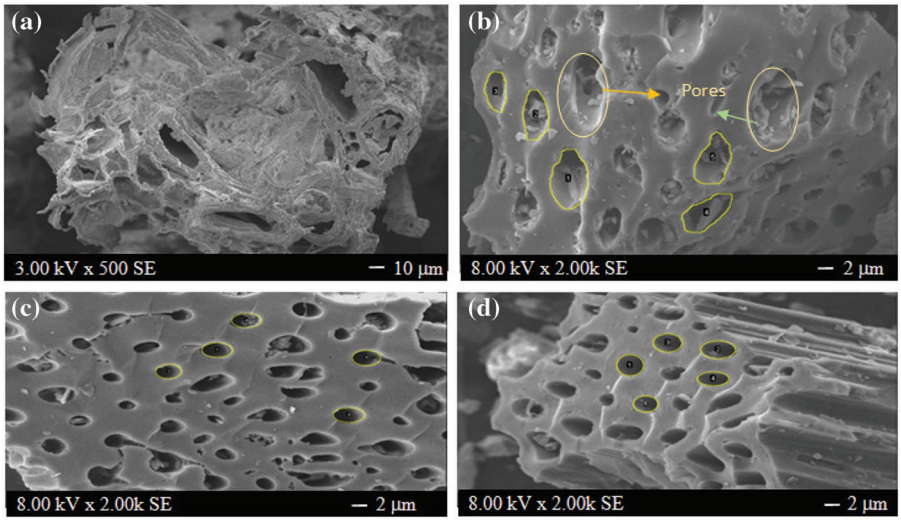


**Figure 2:** Morphology of 500× magnification of palm fronds (a), 2000× magnification after carbonization (b), $H_3PO_4$ activation (c), and KOH activation (d)

Inactivated carbon has an irregular pore structure, and it appears that a lot of impurities are still present. Carbonization also decomposes organic matter and removes volatile substances so that there is a rearrangement of the structure at the end of the process; the surface of the charcoal after carbonization looks rough because there are impurities in the form of hydrocarbons, tar, and other compounds, causing the charcoal pores to close.

Figs. 2c and 2d show that $H_3PO_4$ and KOH activators play a role in forming a porous surface on the sample having carbon content. Carbon activated with $H_3PO_4$ and KOH shows pores that are more regular and cleaner than those with impurities. The activation process aims to facilitate a reaction between the activator and carbon, which will oxidize and erode hydrocarbons, tar, and other compounds attached to the surface of the charcoal so that the surface of the charcoal becomes smooth and forms new pores. Reduction of the hydrocarbon compounds results in an increased visibility of the surface of the activated carbon. Through activation process, the pores are enlarged by disruption of the hydrocarbon bonds or oxidation of the surface molecules so that the carbon undergoes a change, namely, the surface area increases and affects the adsorption power. However, there is a difference in the pore structure of $H_3PO_4$- and KOH-activated carbon. In activated carbon with $H_3PO_4$ activator, more pores are formed that have cavities with a larger size when compared with KOH-activated carbon. At optimum conditions, the activated carbon of nipa palm fronds shows the presence of quite a large number of pores and the presence of some pores with wide diameters, as shown in Table 2.

**Table 2:** Activated carbon pore diameter (μm)

| Treatment | Diameter (μm) | | |
|---|---|---|---|
| | $D_{min}$ | $D_{max}$ | $D_{ave}$ |
| Carbonization | 1.712 | 13.434 | 7.323 ± 2.866 |
| KOH activation | 1.086 | 6.607 | 3.993 ± 1.086 |
| $H_3PO_4$ activation | 1.640 | 5.504 | 3.720 ± 1.057 |

Carbonization leads to the formation of carbon pores of various sizes, with an average pore diameter of 7.323 ± 2.866 μm. Each pore still contains a lot of impurities, so the activation process with KOH and $H_3PO_4$ continues. Figs. 2c and 2d show that the use of KOH and $H_3PO_4$ activators reduced the impurities in activated carbon and also made the pore more uniform. Pores with diameters 3.720 ± 1.057 μm and 3.993 ± 1.086 μm yielded, respectively, after KOH and $H_3PO_4$ activation. The pore size of the activated carbon determines whether or not a molecule can enter the pore [8]. It is known that the pore diameter and the amount of impurities affect the adsorbent properties of the activated carbon; therefore, the activation process is very necessary.

In general, lignin is able to maintain the morphological structure of biomass because it contains esters and ethers with cross-links, but after the activation process, the lignin structure and cell walls are destroyed, so the pores formed from activated carbon do not have a distinctive shape or are similar to the morphological structure of the raw material. The formation of pores or the expansion of pores into larger pores is caused by reduced impurities on the carbon surface [8]. The activation process causes many volatile compounds to be released, thereby opening the carbon pores and reducing the closure of the hydrocarbons. The formation and enlargement of pores is due to the evaporation of degraded cellulose components. This result is confirmed by the FTIR Spectra data in Fig. 3.

Table 3 shows the change in weight percent of the chemical components of the nipa palm frond samples and after the carbonization and the activation processes with acids and bases. The weight percent of C increased after activation, while activation with $H_3PO_4$ acid activator showed the highest results. These results prove that because of the carbonization and activation processes the value of the carbon content increases and the impurities contained in the nipa palm frond samples are removed.

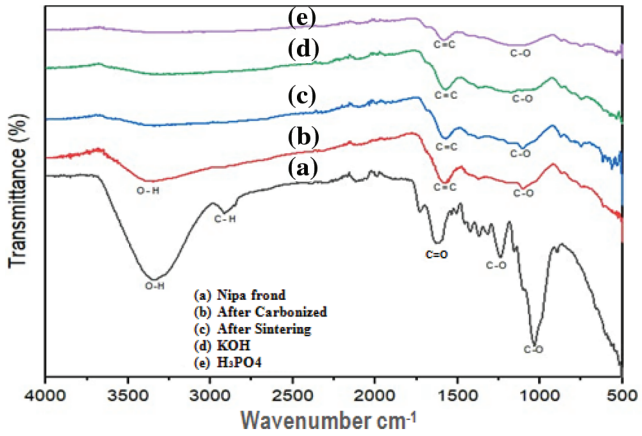


**Figure 3:** FTIR spectra of activated carbon Nipa palm fronds

**Table 3:** Activated carbon elemental content with SEM EDX (energy dispersive X-ray)

| Element | Nipa frond | | Carbonization | | KOH activation | | $H_3PO_4$ activation | |
|---|---|---|---|---|---|---|---|---|
| | Wt % | At. % | Wt % | At. % | Wt % | At. % | Wt % | At. % |
| C | 22.26 | 30.36 | 47.76 | 61.81 | 52.97 | 60.58 | 53.45 | 61.05 |
| N | 3.61 | 4.22 | 4.74 | 5.26 | 11.61 | 11.39 | 9.53 | 9.34 |
| O | 50.3 | 51.5 | 17.01 | 16.53 | 28.95 | 24.85 | 31.48 | 26.99 |
| Na | 10.37 | 7.39 | 11.55 | 7.81 | 1.29 | 0.77 | – | – |
| Mg | 1.02 | 0.69 | 1.01 | 0.65 | 1.37 | 0.77 | 1.09 | 0.62 |
| Al | 0.29 | 0.18 | 0.23 | 0.13 | – | – | 0.66 | 0.34 |
| Si | 0.79 | 0.46 | 0.51 | 0.28 | 1.31 | 0.64 | 1.35 | 0.66 |
| P | 0.38 | 0.2 | 0.77 | 0.39 | 1.21 | 0.54 | 1.35 | 0.6 |
| S | 0.69 | 0.35 | 0.69 | 0.33 | – | – | – | – |
| Cl | 8.24 | 3.81 | 13.67 | 6 | – | – | 1.08 | 0.42 |
| K | 1.28 | 0.54 | 2.06 | 0.82 | 1.29 | 0.45 | – | – |
| Ca | 0.77 | 0.31 | – | – | – | – | – | – |

### *3.3 Functional Group Identification*

The process of changing chemical bonds in each process is also indicated by the results of the FTIR measurement. The functional groups of nipa palm fronds are shown in Fig. 3a. The typical peaks of lignin, hemicellulose, and cellulose constituent groups are indicated by the wave number 3333 $cm^{-1}$, which is associated with the O-H strain on cellulose [26]. The 2917 $cm^{-1}$ peak indicates the C-H strain on the methyl and methylene groups found in lignin and cellulose [27], while the 1737 $cm^{-1}$ wave peak represents the C=O stretching vibration on hemicellulose [28]. The peak of 1609–1635 $cm^{-1}$ is associated with the stretching vibrations of C=O and C=C in lignin [29]. The 1422 $cm^{-1}$ peak indicates C-H deformation in lignin [30], while the 1370 $cm^{-1}$ peak corresponds to the C-H deformation in lignin, cellulose, and hemicellulose [31]. The typical lignin peak is in the range of wave number 1234 $cm^{-1}$, which is indicated

by the C=O stretching vibration [32], while the 1032 $cm^{-1}$ peak is associated with the C-O vibration on cellulose [33] and the 897 $cm^{-1}$ peak with the C-H deformation in cellulose and hemicellulose [32].

Carbonization, sintering, and activation of KOH and $H_3PO_4$ reduced the levels of lignin and other chemical extracts and increased the levels of cellulose. This is shown by the results of the FTIR spectra of Figs. 3b–3e. It can be seen that there are several missing transmittance peaks, namely, 2917 $cm^{-1}$ and 1635 $cm^{-1}$, where these two groups are lignin component compounds. Likewise, the wave crest around 1234–1449 $cm^{-1}$, which is typical for lignin, was also lost. The treatment of KOH and $H_3PO_4$ by carbonization, sintering, and activation also caused the peak of wave 1609 $cm^{-1}$ to shift to a smaller wave number, which indicates that activated carbon was formed, which is the hexagonal carbon C=C group. This indicates that there was a reaction between the chemical components of the nipa frond during carbonization of KOH and $H_3PO_4$. Likewise, the wave peak of 1737 $cm^{-1}$ disappeared after the sample was carbonized, sintered, and activated. This indicates that there was a release of hemicellulose components in the palm fronds. Wave number 1609 $cm^{-1}$ shifted to wave number 1578 and 1570 $cm^{-1}$ after carbonization and sintering, and activation of KOH and $H_3PO_4$, respectively, at 1570 $cm^{-1}$. This shows that C=O and C=C stretching vibrations in lignin [29] are still present, although it indicates a chemical reaction took place as the presence of C=C groups shows an increase in carbon content. The C=O group is a typical group found in activated carbon and shows that the palm frond has formed an active carbon substance.

The decrease in OH compounds was also significantly reduced due to this treatment, which can be seen at the peak of 3333 $cm^{-1}$. This shows that the OH bonds were released during the process. At the time of carbonization and sintering, this peak shifted to around 3351 and 3345 $cm^{-1}$, and after the activation process of KOH and $H_3PO_4$, it shifted to around 3341 and 3331 $cm^{-1}$. The shift of the O-H groups tends to originate from the reaction between the activator and the free compound on the activated carbon surface. The functional groups on the surface of activated carbon that are activated form polar-activated carbon.

The peak intensity of 1032 $cm^{-1}$ showed that the C-O vibrations in cellulose [33] also decreased and shifted to a larger wave number; this indicated that cellulose deformation had occurred in the carbon of the palm fronds. Likewise, the peak of 897 $cm^{-1}$ shifted to a smaller wave number, indicating that deformation had occurred in cellulose and hemicellulose [32]. Based on the identification of functional groups with the FTIR spectrophotometer, it is seen that the active carbon of the nipa palm fronds was dominated by the C=O, C=C, C-C, and C-H groups.

### *3.4 Activated Carbon Adsorption Ability*

Swamp or peat water contains various metals, so before it is utilized, it needs to be treated; one of the methods for treating it includes the adsorption of the metal elements. Activated carbon is a material that has a high adsorption capacity, so it can be used to improve the water quality. Before investigating the adsorption capacity of the activated carbon, the adsorption process by filter paper was observed first. The Fe level in peat water was found to be in the range 1.08–1.83 mg/L. Table 4 shows that the Fe level reduced after the peat water was passed through the filter paper. However, it seems that some amount of Fe was retained on the filter paper.

**Table 4:** Fe reduction efficiency of filter paper

| Point | Control 1 (mg/L) | Control 2 (mg/L) | Difference (mg/L) | Fe reduction efficiency (%) |
|---|---|---|---|---|
| 1 | 1.83 | 1.52 | 0.31 | 16.94 |
| 2 | 1.08 | 0.84 | 0.24 | 22.22 |
| 3 | 1.78 | 1.68 | 0.1 | 5.62 |

Note: Control 1 = Concentration before filtering.
Control 2 = Concentration after filtering.

The reduction of the Fe level in peat water with the use of activated carbon, obtained from nipa palm fronds with different activators, is shown in Table 5. Nipa palm frond-activated carbon with $H_3PO_4$ activator reduced Fe levels by 39.23% with an adsorption capacity of 0.76 mg/g, while that with KOH activator reduced Fe levels by 22.82% with an adsorption capacity of 0.45 mg/g.

**Table 5:** Fe reduction efficiency and adsorption capacity

| Activator | Sample | Control 1 (mg/L) | Control 2 (mg/L) | Fe reduction efficiency (%) | Adsorption capacity (mg/g) |
|---|---|---|---|---|---|
| KOH | A1 | 1.83 | 1.43 | 21.86 | 0.49 |
| | A2 | 1.08 | 0.88 | 18.52 | 0.25 |
| | A3 | 1.78 | 1.28 | 28.09 | 0.62 |
| | Average | 1.56 | 1.20 | 22.82 | 0.45 |
| $H_3PO_4$ | B1 | 1.83 | 1.15 | 37.16 | 0.84 |
| | B2 | 1.08 | 0.85 | 21.30 | 0.28 |
| | B3 | 1.78 | 0.85 | 52.25 | 1.15 |
| | Average | 1.56 | 0.95 | 39.23 | 0.76 |

Note: Control 1 = Concentration before filtering.
Control 2 = Concentration after filtering.

This occurred because of the adsorption process of Fe metal on the activated carbon surface, which occurs due to the van der Waals force, due to which the pores of the activated carbon will attract pollutant particles and be trapped [8]. The smaller the particle size of the activated carbon that is formed, the greater the surface contact, which in turn increases the likelihood of the adsorbate sticking to the porous surface of the activated carbon. Then the Fe removal efficiency will be higher. This was confirmed by the results of the analysis of surface morphology and the pore size of the activated carbon using SEM as shown in Fig. 2 and Table 3. The pore diameter of the activated carbon with the $H_3PO_4$ activator is larger than that with KOH. Therefore, the Fe reduction efficiency of the $H_3PO_4$-activated carbon is also better than the KOH one.

## 4 Conclusion

Using the pyrolysis method, activated carbon was successfully produced from palm fronds. The characteristics of activated carbon, which include moisture content, ash content, volatile matter content, and fixed carbon, were determined, and the results complied with SNI No. 06-3730-1995. Activated carbon with $H_3PO_4$ activator reduced Fe levels by 39.23% with a capacity to reduce Fe by 0.76 mg/g, while KOH activator reduced Fe levels by 22.82% with a capacity to reduce Fe by 0.45 mg/g.

**Acknowledgement:** The authors would like to thank to everyone who have provided a lot of support in completing this research, especially the Materials Physics Expertise Group, Physics Study Program, FMIPA, University of Lambung Mangkurat.

**Funding Statement:** The authors received no specific funding for this study.

**Author Contributions:** The authors confirm contribution to the paper as follows: study conception and design: N. H. Haryanti, Suryajaya; data collection: Nurlita Sari; analysis and interpretation of results: Eka Suarso, Tetti N. Manik, Suryajaya; draft manuscript preparation: N. H. Haryanti, Suryajaya, Darminto. All authors reviewed the results and approved the final version of the manuscript.

**Availability of Data and Materials:** The authors confirm that the data supporting the findings of this study are available within the article.

**Conflicts of Interest:** The authors declare that they have no conflicts of interest to report regarding the present study.

## References


1. Econusa (2021). Let's get to know the importance of peatlands! https://econusa.id/en/ecodefender/lets-get-to-know-the-importance-of-peatlands/ (accessed on 09/11/23)
2. Lubis, K. L., Elystia, S., Ermal, D. A. S., Zultiniar, Z. (2022). Removal of Fe from peat water using chitosan membrane as adsorbent. *Jurnal Sains Teknologi & Lingkungan, 8(1),* 15–24. https://doi.org/10.29303/jstl.v8i1.298
3. Setiasih, J. (2010). *Analysis of iron (Fe), copper (Cu), and calcium (Ca) levels in peat water after being clarified using the electrocoagulation method (Thesis)*. USU University, USA. https://repositori.usu.ac.id/handle/123456789/36977 (accessed on 09/11/23)
4. Benalia, A., Derbal, K., Khalfaoui, A., Pizzi, A., Medjahdi, G. (2022). The use of aloe vera as natural coagulant in algerian drinking water treatment plant. *Journal of Renewable Materials, 10(3),* 625–637. https://doi.org/10.32604/jrm.2022.017848
5. Abou-Zeid, R. E., Ali, K. A., Gawad, R. M. A., Kamal, K. H., Kamel, S. et al. (2021). Removal of Cu(II), Pb(II), Mg(II), and Fe(II) by adsorption onto alginate/nanocellulose beads as bio-sorbent. *Journal of Renewable Materials, 9(4),* 601–613. https://doi.org/10.32604/jrm.2021.014005
6. Nizam, N. U. M., Hanafiah, M. M., Noor, I. M., Karim, H. I. A. (2020). Efficiency of five selected aquatic plants in phytoremediation of aquaculture wastewater. *Applied Sciences, 10(8)*. https://doi.org/10.3390/APP10082712
7. Syauqiah, I., Elma, M., Mailani, D. P., Pratiwi, N. (2020). Activated carbon from nypa (Nypa fruticans) leaves applied for the Fe and Mn removal. *IOP Conference Series: Materials Science and Engineering, 980,* 012073. https://doi.org/10.1088/1757-899X/980/1/012073
8. Reza, M. S., Yun, C. S., Afroze, S., Radenahmad, N., Bakar, M. S. A. et al. (2020). Preparation of activated carbon from biomass and its' applications in water and gas purification, a review. *Arab Journal of Basic and Applied Sciences, 27(1),* 208–238. https://doi.org/10.1080/25765299.2020.1766799
9. Heidarinejad, Z., Dehghani, M. H., Heidari, M., Javedan, G., Ali, I. et al. (2020). Methods for preparation and activation of activated carbon: A review. *Environmental Chemistry Letters, 18(2),* 393–415. https://doi.org/10.1007/s10311-019-00955-0
10. Tohamy, H. A. S., El-Sakhawy, M., Kamel, S. (2022). Development of magnetite/graphene oxide hydrogels from agricultural wastes for water treatment. *Journal of Renewable Materials, 10(7),* 1889–1909. https://doi.org/10.32604/jrm.2022.019211
11. Mulana, F., Mariana, M., Muslim, A., Mohibah, M., Halim, K. H. K. (2018). Removal of zinc (II) ion from aqueous solution by adsorption onto activated palm midrib bio-sorbent. *IOP Conference Series: Materials Science and Engineering, 334(1),* 012027. https://doi.org/10.1088/1757-899X/334/1/012027
12. Astuti, M. D., Nisa, K., Mustikasari, K. (2020). Identification of chemical compounds from nipah (*Nypa fruticans Wurmb*.) endosperm. *BIO Web of Conferences, 20,* 03002. https://doi.org/10.1051/bioconf/20202003002
13. Cheablam, O., Chanklap, B. (2020). Sustainable nipa palm (*Nypa fruticans* Wurmb.) product utilization in Thailand. *Scientifica, 2020,* 1–10. https://doi.org/10.1155/2020/3856203
14. Zakaria, U. M., Faslih, A., Umar, M. (2018). Usage period of nipah leaves nypa fructicans with salt water treatment as roofing material. *E3S Web Conference, 67,* 4–6. https://doi.org/10.1051/e3sconf/20186704001
15. Akpakpan, A. E., Akpabio, U. D., Obot, I. B. (2012). Evaluation of physicochemical properties and soda pulping of Nypa fruticans frond and petiole. *Applied Chemistry, 45,* 7664–7668. https://www.researchgate.net/publication/303155607_Evaluation_of_physicochemical_properties_and_soda_pulping_of_Nypa_fruticans_frond_and_petiole/link/5796eddc08ae33e89fad8de4/download (accessed on 09/11/23)

16. Mariana, M., Mistar, E. M., Aswita, D., Zulkipli, A. S., Alfatah, T. (2023). Nipa palm shell as a sustainable precursor for synthesizing high-performance activated carbon: Characterization and application for $Hg^{2+}$ adsorption. *Bioresource Technology Reports, 21,* 101329. https://doi.org/10.1016/j.biteb.2022.101329
17. Maulina, S., Iriansyah, M. (2018). Characteristics of activated carbon resulted from pyrolysis of the oil palm fronds powder. *IOP Conference Series: Materials Science and Engineering, 309(1),* 012072. https://doi.org/10.1088/1757-899X/309/1/012072
18. Wibowo, I. A., Sulistyo, S., Suprihanto, A. (2022). Making porous graphite electrodes for the electrolysis process. *Jurnal Teknik Mesin, 10(4),* 497–502. https://ejournal3.undip.ac.id/index.php/jtm/article/view/36136 (accessed on 09/11/23)
19. Taslim, I., Bani, O., Audina, E., Hidayat, R. (2021). Preparation of activated carbon-based catalyst from nipa palm (*Nypa fruticans*) shell modified with KOH for biodiesel synthesis. *IOP Conference Series: Earth and Environmental Science, 912(1),* 012094. https://doi.org/10.1088/1755-1315/912/1/012094
20. Sa'diyah, K., Suharti, P. H., Hendrawati, N., Pratamasari, F. A., Rahayu, O. M. (2021). Utilization of wood sawdust as active carbon through pyrolysis and chemical activation processes. *CHEESA: Chemical Engineering Research Articles, 4(2),* 91. https://doi.org/10.25273/cheesa.v4i2.8589.91-99
21. Syabana, D. K., Widiastuti, R. (2018). Physical characteristics of palm fiber (*Nypa fruticans*). *Dinamika Kerajinan dan Batik Majalah Ilmiah, 35(1),* 9. https://doi.org/10.22322/dkb.v35i1.3771
22. Esterlita, M. O., Herlina, N. (2015). The effect of adding $ZnCl_2$, KOH, and $H_3PO_4$ activators in making active carbon from palm fronds (*Arenga pinnata*). *Jurnal Teknik Kimia USU, 4(1),* 47–52. https://doi.org/10.32734/jtk.v4i1.1460
23. Hendrawan, Y., Sutan, S. M., Kreative, R. Y. R. (2017). The effect of variations in carbonization temperature and activator concentration on the characteristics of activated carbon from bagasse using the activating agent NaCl. *Jurnal Keteknikan Pertanian Tropis Dan Biosistem, 5(3),* 200–207. https://jkptb.ub.ac.id/index.php/jkptb/article/view/420/349 (accessed on 09/11/23)
24. Fauzia, E. A., Purnama, H. (2021). The effect of particle size on the characterization of activated carbon from tropical black bamboo (*Gigantochloa atroviolacea*). *Techno, 22(2),* 99. https://doi.org/10.30595/techno.v22i2.10350
25. Suryajaya, Haryanti, N. H., Husain, S., Safitri, M. (2020). Preliminary study of activated carbon from water chestnut (*Eleocharis dulcis*). *Journal of Physics: Conference Series, 1572,* 012053. https://doi.org/10.1088/1742-6596/1572/1/012053
26. Nang An, V., Chi Nhan, H. T., Tap, T. D., Van, T. T. T., Van Viet, P. et al. (2020). Extraction of high crystalline nanocellulose from biorenewable sources of Vietnamese agricultural wastes. *Journal of Polymers and the Environment, 28(5),* 1465–1474. https://doi.org/10.1007/s10924-020-01695-x
27. Pinheiro, N. P. F., Barros, N. E. L. (2021). Steam explosion: Hydrothermal pretreatment in the production of an adsorbent material using coconut husk. *Bioenergy Research, 14(1),* 153–162. https://doi.org/10.1007/s12155-020-10159-y
28. Shamsuddin, M. S., Yusoff, N. R. N., Sulaiman, M. A. (2016). Synthesis and characterization of activated carbon produced from kenaf core fiber using $H_3PO_4$ activation. *Procedia Chemistry, 19,* 558–565. https://doi.org/10.1016/j.proche.2016.03.053
29. Cheng, J., Yue, L., Ding, L., Li, Y. Y., Ye, Q. et al. (2019). Improving fermentative hydrogen and methane production from an algal bloom through hydrothermal/steam acid pretreatment. *International Journal of Hydrogen Energy, 44(12),* 5812–5820. https://doi.org/10.1016/j.ijhydene.2019.01.046
30. Horikawa, Y., Hirano, S., Mihashi, A., Kobayashi, Y., Zhai, S. et al. (2019). Prediction of lignin contents from infrared spectroscopy: Chemical digestion and lignin/biomass ratios of *Cryptomeria japonica*. *Applied Biochemistry and Biotechnology, 188(4),* 1066–1076. https://doi.org/10.1007/s12010-019-02965-8
31. Liu, Y., Liu, A., Ibrahim, S. A., Yang, H., Huang, W. (2018). Isolation and characterization of microcrystalline cellulose from pomelo peel. *International Journal of Biological Macromolecules, 111,* 717–721. https://doi.org/10.1016/j.ijbiomac.2018.01.098

32. Gonultas, O., Candan, Z. (2018). Chemical characterization and FTIR spectroscopy of thermally compressed eucalyptus wood panels. *Maderas: Ciencia Y Tecnologia, 20(3),* 431–442. https://doi.org/10.4067/S0718-221X2018005031301
33. Kang, C., Zhu, L., Wang, Y., Wang, Y., Xiao, K. et al. (2018). Adsorption of basic dyes using walnut shell-based biochar produced by hydrothermal carbonization. *Chemical Research in Chinese Universities, 34(4),* 622–627. https://doi.org/10.1007/s40242-018-8018-0